Research on Engineering Structures & Materials
journal homepage: http://www.jresm.org
MIM Research Group

Research Article

Evaluation of mechanical properties for banana-carbon fiber reinforced nano-clay epoxy composite using analytical modeling and simulation

Tanvi Saxena*[a], V.K. Chawla[b]

Department of Mechanical and Automation Engineering, Indira Gandhi Delhi Technical University for Women, Kashmere Gate, Delhi, India

Article Info

Article history:

Received 19 Feb 2022
Revised 18 Jun 2022
Accepted 17 Aug 2022

Keywords:

Analytical models;
Composite material;
Effective elastic properties;
Nano-clay;
Natural fibers

Abstract

Nano-fillers are bringing impeccable development in the area of materials science and natural fibers reinforced composites. In this study, a composite consisting of banana-carbon fiber reinforced epoxy matrix filled with 1%, 3%, and 5% weight percentage of nano-clay particles (NC) and carrying a transverse load is investigated for its mechanical and elastic properties. Nano-clay layer with interphase are arranged in layers called nano-clay platelets. The elastic properties such as longitudinal elastic modulus, transverse elastic modulus, in-plane Poisson's ratio, in-plane and out-of-plane shear modulus for the proposed composite are calculated by using different analytical models namely, Mori-Tanaka, Bridging, Generalized Self-Consistent, and Modified Halpin-Tsai model. The strength and deformation of the proposed composite are analyzed by using the ANSYS APDL application. The proposed composite is modeled using two layers of banana fibers, two layers of carbon fiber, and one layer of nano-clay platelet. The fibers and nano-clay platelet are arranged in a specific sequence of banana fiber at 90^0, carbon fiber at 0^0, nano-clay platelet at 90^0, carbon fiber at 0^0, and banana fiber at 90^0. The proposed composite reinforced with 3% nano-clay is showing the least deformation as compared to 1% and 5% reinforcement. It is also observed that the modified Halpin-Tsai model outperforms all the other models as it is yielding the most effective elastic properties for the proposed composite and Mori-Tanaka model is found to be the least effective model for the calculation of elastic features of the proposed composite. Additionally, the hybridization effect for the composite is also calculated to analyze the tensile failure strain characteristics for banana and carbon fibers in the hybrid composite.

1. Introduction

Banana fibers come under the category of bast fibers and find applications in automobile and aviation industries due to their availability, high rigidness, and fire-defiant features [1-3, 10]. Natural fibers reinforced green composites are being extensively used these days due to their excellent features and eco-friendly aspect [15, 16]. For attaining sustainable development, Green Operations Management (GOM) is gaining wide attention from community [32]. Banana fibers blended with carbon fibers reinforced composites improves ductility and imparts high degree of flexibility. Carbon fibers due to their high strength and lightweight attributes find wide applications in aerospace, cycles, motorcycles, etc., where high strength-to-weight ratios are required [4]. Research has been carried out on enhancing the physical features of composites. Mechanical features of the composite like tensile, bending, and crushing strength get enhanced by increasing the core diameter of the composite structure [5]. A new invariant-based technique for

*Corresponding author: tanvi002phd18@igdtuw.ac.in
*[a] orcid.org/0000-0002-3229-6294; [b]orcid.org/0000-0001-7386-1838
DOI: http://dx.doi.org/10.17515/resm2022.403me0219
Res. Eng. Struct. Mat. Vol. x Iss. x (xxxx)xx-xx

describing the elastic features and failure of composites and laminates was found to be commendable in enhancing the design and manufacturing of carbon/epoxy composites [27, 28].

In the past few decades, nano-composites have witnessed a tremendous growth in gaining the attention of researchers. It is observed that among various nano-fillers reinforced natural fiber composites, the most favorable and encouraging nano-composite could be the one reinforced with nano-clay consisting of silicate MMT(montmorillonite) layers [4, 6]. Nano-clays have certain remarkable features like large aspect ratio and large surface exposure that can improve the mechanical features of the polymer. The infusion of 6 wt% of nano-clay particles into banana fibers with the help of alkaline (NaOH) chemical analysis gives superior tensile, thermal, and interfacial properties as compared to untreated banana fibers. A threefold rise in tensile modulus and a 53% rise in tensile strength were noticed in nano-clay-blended treated banana fibers over untreated banana fibers [7]. The nano-clay particles blended banana fibers blended epoxy polymer composites resulted in a rise of 25% in Young's modulus, 11% in yield stress, and 26% in ultimate tensile strength when compared with untreated banana fibers blended epoxy composite [8]. The mechanical strength of nano-clay filled carbon fiber reinforced interpenetrating polymer networks (IPN) matrix composite was studied by varying the percentage of nano-clay to 0%, 1%, 3%, 5%, 7% & 9%. The inclusion of nano-clay enhances the mechanical strength of the composite to many folds but only up to 5% nano-clay addition. Beyond that, 7% and 9% nano-clay infusion showed a decline in mechanical strength [9].

The factors that affect the structure of nanomaterials are very complicated. The factors include the substance type, particle size, arrangement of nano-crystals, and preparation methods. The structure of nanomaterials can be divided into two categories: the first type is composed of two forms of structure that consist of particles and grain boundaries, and all structural components have the size in nanometers [11]. The second type of nanomaterial has a less dense random network of structure material having numerous nano-sized cavities. The whole layout has nano crystalline fragments and nano systems. A continuum non-local modified gradient theory was proposed and found to be suitably implemented for examining nanoscopic static and dynamic behaviour of nano-sized elastic beams [17]. A non-local gradient theory of elasticity theory was proposed which found to be beneficially employed in the severe analysis of nano-technological devices [18]. A higher order elasticity theory was found to be utilized effectively for characterizing advanced nano-materials and structural components of nano-systems [19]. The non-local modified gradient elasticity theory was found to be suitable for providing a practical outlook to the nanoscopic examination of the field variables [20].

Numerical method approach have been used by the researchers for evaluating Young's modulus of a nano-clay particle blended nano-composite [21], simulation methods [22-25], or using both together [26]. Numerical procedures are being opted more nowadays due to the advancement of computational techniques; however analytical methods are always preferred first for multivariable problems [26, 31]. Experimental work has other limitations also like, considering all aspects of well-defined systems, like particle dimensions, particle distribution, and shape arrangements. The mechanical features of composites can be achieved better using analytical modeling methods [29]. Continuum micromechanical models like Halpin-Tsai [12], ROM [13, 14, 30], have been used successfully for determining equivalent elastic properties of polymer silicate nano-composites and structural study of micro composites.

From the above literature, it is evident that the composite of banana-carbon fiber and epoxy matrix blended with nano-clay particles had never been explored for its elastic and

mechanical properties. Also, the value of the hybridization effect for the proposed composite has never been calculated before by any researcher. Therefore, to bridge the aforementioned research gaps, in this paper following research problems are addressed.

- A new composite banana-carbon fiber reinforced epoxy matrix filled with different weight percentages of nano-clay particles carrying a transverse load of 200KN (along -z direction) is modeled in ANSYS APDL.
- The elastic and mechanical features for the newly proposed composite are calculated by employing the Mori-Tanaka, Bridging, Generalized Self-Consistent, and Modified Halpin-Tsai model.
- The strength and deformation of the proposed composite reinforced with 1%, 3%, and 5% of nano-clay particles are analyzed at different orientation angles by using the ANSYS APDL application.
- The hybridization effect for the composite is also calculated to analyze the tensile failure strain for high and low elongation fibers for the proposed composite.

2. Background

2.1. Modeling of the Banana-Carbon Fiber-Reinforced Nano-Clay Epoxy Composite

The layers of banana fiber, carbon fiber, and nano-clay layers along with interphase are arranged to form a sandwich intercalated composite structure. Epoxy is used as a matrix. Intercalated nano-composite has a single layer of interphase, while exfoliated has two. Clay particles are arranged in layers composed of silicate platelets (having nano-thickness) and an interphase layer. The interphase layer is naturally developed due to physical interactions between the nano-clay and polymer matrix [71]. Nano-clay platelet is 0.5mm thick and length of the nano-clay platelet and interphase are considered as same (Fig. 2). The average particle size of nano-clay particles is between 50-100nm [33].

Both numerical homogenization and analytical models have been used consequently for determining the mechanical features of the nano-composite [16, 34]. Depending upon the structure and chemical constitution of nano-particles, nano-clay can be classified into various categories like illite, bentonite, kaolinite, and montmorillonite. Homogenization micromechanical models like Mori-Tanaka (M-T) [35, 36, 67], self-consistent [37, 34], and Lielen's model [38] have been employed for computing various properties of short fiber composites. Self-consistent and Mori-Tanaka models were employed for short fiber composites and the M-T model was found to give the best values for fillers with a large aspect ratio. For higher fiber volume fractions and strength parameters, Lielen's model [38] proved to be better than the M-T model.

3. Analytical Modeling Methods

The proposed composite is designed using semi-empirical and homogenization models, by varying the composition percentage of nano-clay and epoxy while keeping the percent weight of banana and carbon fiber fixed as given in Table 1. The elastic features of carbon and banana fiber, epoxy, and nano-clay are given in Table 2. The volume fractions of the fibers, matrix, and filler are evaluated using the following equations [3] and are given in Table 3. The volume fraction of the interphase is about one percent of the volume fraction of the nanoparticle [72].

$$V_{fb/mx/NC} = \frac{W_{fb/mx/NC}}{\rho_{fb/mx/NC}} \times \rho_C \tag{1}$$

Where

$$\rho_C = \frac{1}{\frac{W_{CF}}{\rho_{CF}} + \frac{W_{BF}}{\rho_{BF}} + \frac{W_{EP}}{\rho_{EP}} + \frac{W_{NC}}{\rho_{NC}}} \quad (2)$$

3.1. Homogenization Models

Analytical homogenization models depend on the comprehensive mechanical performance of the composite structure that belongs to the macroscopic frame and heterogeneous microscopic frame of materials (e.g. composition, properties, shape, volume fraction, inclination, etc.) [45]. Homogenization models aim to obtain the stress, and strain behavior at the microscopic and macroscopic frames [46, 47].

3.1.1. Mori-Tanaka Model

The Mori-Tanaka model was originally formed by [35]. This model is reckoned for developing various kinds of composite systems. This model uses the theory of Eshelby inclusion. The aim is to define the average behaviors of the fiber and matrix. As reported in [48], the longitudinal and transverse Young's moduli, in & out-of-plane moduli of rigidity, and in-plane Poisson's ratio is given by equations.

Table 1. Weight percentages of fibers, matrix, and nano-clay

Sequence	Banana fiber (%)	Carbon fiber (%)	Epoxy (%)	Nano-clay (%)
I	20	60	19	1
II	20	60	17	3
III	20	60	15	5

Table 2. Elastic features of fibers, matrix, nano-clay, and interphase

Properties	Carbon fiber [42]	Banana fiber [42]	Epoxy [43]	Nano-clay [44]	Interphase [44]
${E_1}^{fb/mx}$ = (GPa)	230	3.48	35	$E_{NC} = 176$	$E_{IP} = 11.6$
${E_{22}}^{fb} = {E_{33}}^{fb}$ (GPa)	15	---	---	---	---
${G_{12}}^{fb/mx} = {G_{13}}^{fb/mx}$ (GPa)	15	1.58	0.32	$G_{NC} = 70.4$	$G_{IP} = 4.55$
${G_{23}}^{fb}$ (GPa)	7	---	---	---	---
${\upsilon_{12}}^{fb/mx} = {\upsilon_{31}}^{fb/mx}$	0.2	0.28	0.35	$\upsilon_{NC} = 0.25$	$\upsilon_{IP} = 0.275$
${\upsilon_{23}}^{fb}$	0.07	---	---	---	---
$\rho^{fb/mx}$ (kg/m³)	2260	1350	1270	1980	1590

Table 3. Evaluated volume fractions of the fibers, matrix, nano-clay, and interphase

Sequence	Carbon (CF)	Banana (BF)	Epoxy	Nano-clay (NC)	Interphase (IP)
	V_{CF}	V_{BF}	V_{EP}	V_{NC}	V_{IP}
I	0.47	0.26	0.26	8.89×10^{-3}	8.89×10^{-5}
II	0.47	0.26	0.24	0.027	2.7×10^{-4}
III	0.48	0.27	0.21	0.045	4.53×10^{-4}

$$E_1 = V_{fb}{E_1}^{fb} + (1 - V_{fb})E^{mx} + 2V_{fb}(1 - V_{fb})Z_1({\upsilon_{12}}^{fb} - \upsilon^{mx})^2 \quad (3)$$

$$E_2 = \frac{E_1}{[1 - (\upsilon^{mx})^2](Y_1 + Y_2)} \quad (4)$$

$$\upsilon_{12} = \upsilon^{mx} + 2V_{fb}\frac{Z_1}{E^{mx}}(\upsilon_{12}{}^{fb} - \upsilon^{mx})[1 - (\upsilon^{mx})^2] \tag{5}$$

$$G_{12} = \frac{E^{mx}}{2(1 - V_{fb})(1 + \upsilon^{mx})}\left[1 + V_{fb} - \frac{4V_{fb}}{1 + V_{fb} + 2(1 - V_{fb})\frac{G_{12}{}^{fb}}{E^{mx}}(1 + \upsilon^{mx})}\right] \tag{6}$$

$$G_{23} = E^{mx}\left[2\left(1+\upsilon^{mx}\right) + \frac{V_{fb}}{\frac{1-V_{fb}}{8[1-\left(\upsilon^{mx}\right)^2]} + \frac{G_{23}{}^{fb}}{E^{mx} - 2G_{23}{}^{fb}\left(1+\upsilon^{mx}\right)}}\right]^{-1} \tag{7}$$

Where:

$$Y_1 = V_{fb}Z_1\left(\frac{E_1{}^{fb}}{E^{mx}}\right)\left[\frac{1 + \upsilon^{mx}}{E^{mx}} - \frac{2}{E_1{}^{fb}} + \frac{1 + \upsilon_{23}{}^{fb}}{E_2{}^{fb}}\right] \tag{8}$$

$$Y_2 = \frac{1}{1 - (\upsilon^{mx})} + 2V_{fb}\left(\frac{E_1}{Z_2}\right)\left[1 + \upsilon_{23}{}^{fb} - \frac{E_2{}^{fb}}{E^{mx}}(1 - \upsilon^{mx})\right] \tag{9}$$

$$Z_1 = \left\{-2(1 - V_{fb})\frac{(\upsilon_{23}{}^{fb})^2}{E_1{}^{fb}} + (1 - V_{fb})\frac{1 - \upsilon_{23}{}^{fb}}{E_2{}^{fb}} + \frac{(1 + \upsilon^{mx})[1 + V_{fb}(1 - 2\upsilon^{mx})]}{E^{mx}}\right\} \tag{10}$$

$$Z_2 = E_2{}^{fb}(3 + V_{fb} - 4\upsilon^{mx})(1 + \upsilon^{mx}) + (1 - V_{fb})E^{mx}(1 + \upsilon_{23}{}^{fb}) \tag{11}$$

Thus for 1% nano-clay, the elastic features of the banana-carbon fiber-reinforced nano-clay epoxy composite can be evaluated using Eqs. (3)-(7):

$E_1 = 119797.9MPa$

Where: $Z_{1_{CF}} = 16638.9; Z_{1_{BF}} = 52356; Z_{1_{NC}} = 2586.9; Z_{1_{IP}} = 28423.25$ (Values calculated using Eq. (10))

$E_2 = 1.7100 \times 10^{13}MPa; \upsilon_{12} = 0.24$

Where: $Y_{1_{CF}} = 5.2; Y_{2_{CF}} = 4$ (Values calculated using Eq. (8) & (9))

$G_{12} = 13882.08MPa + G_{NCP,12}$
$= 13882.08MPa + 6.92 \times 10^6 = 6.93 \times 10^6 MPa$
$G_{23} = 10485.6MPa + G_{NCP,23}$
$= 10485.6MPa + 6.92 \times 10^6 MPa = 6.93 \times 10^6 MPa$

Likewise, similar elastic properties of the proposed composite are evaluated for 3% and 5% nano-clay and are given in Table 4.

3.1.2. Generalized Self-Consistent Model

The generalized self-consistent (GS-C) model was initially evolved by [49, 34] to determine the elastic features of isotropic spherical inclusions blended composite materials. This model can be further utilized to find out the elastic features of short fiber composites [50, 68]. In this model, a particulate having elastic properties of short fiber is supposed to be placed in a homogenous medium, where the surrounding medium has the undetermined elastic features of the composite that requires to be solved.

$$E_1 = {E_1}^{fb}V_{fb} + E^{mx}(1 - V_{fb}) + \frac{4V_{fb}(1 - V_{fb})({\upsilon_{12}}^{fb} - \upsilon^{mx})^2}{\frac{(1-V_{fb})}{{K_{23}}^{fb}} + \frac{V_{fb}}{{K_{23}}^{mx}} + \frac{1}{G^{mx}}} \tag{12}$$

$$\upsilon_{12} = {\upsilon_{12}}^{fb}V_{fb} + \upsilon^{mx}(1 - V_{fb}) + \frac{V_{fb}(1 - V_{fb})({\upsilon_{12}}^{fb} - \upsilon^{mx})\left(\frac{1}{{K_{23}}^{mx}} - \frac{1}{{K_{23}}^{fb}}\right)}{\frac{(1-V_{fb})}{{K_{23}}^{fb}} + \frac{V_{fb}}{{K_{23}}^{mx}} + \frac{1}{G^{mx}}} \tag{13}$$

$$K_{23} = {K_{23}}^{mx} + \frac{V_{fb}}{\frac{1}{{K_{23}}^{fb} - K_{23}} + \frac{1-V_{fb}}{{K_{23}}^{mx} + G^{mx}}} \tag{14}$$

$$G_{12} = G^{mx}\frac{{G_{12}}^{fb}(1 + V_{fb}) + G^{mx}(1 - V_{fb})}{{G_{12}}^{fb}(1 - V_{fb}) + G^{mx}(1 + V_{fb})} \tag{15}$$

$$G_{23} = G^{mx}\left(\frac{-B + \sqrt{B^2 - 4AC}}{2A}\right) \tag{16}$$

Where:

$$A = a_0 + a_1V_{fb} + a_2{V_{fb}}^2 + a_3{V_{fb}}^3 + a_4{V_{fb}}^4 \tag{17}$$

$$B = b_0 + b_1V_{fb} + b_2{V_{fb}}^2 + b_3{V_{fb}}^3 + b_4{V_{fb}}^4 \tag{18}$$

$$C = c_0 + c_1V_{fb} + c_2{V_{fb}}^2 + c_3{V_{fb}}^3 + c_4{V_{fb}}^4 \tag{19}$$

Where:

$$a_0 = -2(G^{mx})^2(2G^{mx} + K^{mx})[2{G_{23}}^{fb}G^{mx} + {K_{23}}^{fb}({G_{23}}^{fb} + G^{mx})\{2{G_{23}}^{fb}G^{mx} + K^{mx}({G_{23}}^{fb} + G^{mx})\}] \tag{20}$$

$$a_1 = 8(G^{mx})^2({G_{23}}^{fb} - G^{mx})[2{G_{23}}^{fb}G^{mx} + {K_{23}}^{fb}({G_{23}}^{fb} + G^{mx})][(G^{mx})^2 + G^{mx}K^{mx} + (K^{mx})^2] \tag{21}$$

$$a_2 = -12(G^{mx})^2(K^{mx})^2({G_{23}}^{fb} - G^{mx})[2{G_{23}}^{fb}G^{mx} + {K_{23}}^{fb}({G_{23}}^{fb} + G^{mx})] \tag{22}$$

$$a_3 = 8(G^{mx})^2[({G_{23}}^{fb}G^{mx})^2{K_{23}}^{fb} + ({G_{23}}^{fb})G^{mx}K^{mx}({K_{23}}^{fb} - G^{mx}) + (K^{mx})^2\{{G_{23}}^{fb}G^{mx}({G_{23}}^{fb} - 2G^{mx}) + {K_{23}}^{fb}({G_{23}}^{fb} - G^{mx})({G_{23}}^{fb} + G^{mx})\}] \tag{23}$$

$$a_4 = 2(G^{mx})^2({G_{23}}^{fb} - G^{mx})(2G^{mx} + K^{mx})[{K_{23}}^{fb}G^{mx}K^{mx} - {G_{23}}^{fb}(2G^{mx}({K_{23}}^{fb} - K^{mx}) + {K_{23}}^{fb}K^{mx})] \tag{24}$$

$$b_0 = 4(G^{mx})^3[2{G_{23}}^{fb}G^{mx} + {K_{23}}^{fb}({G_{23}}^{fb} + G^{mx})][2{G_{23}}^{fb}G^{mx} + K^{mx}({G_{23}}^{fb} + G^{mx})] \tag{25}$$

$$b_1 = 8(G^{mx})^2K^{mx}({G_{23}}^{fb} - G^{mx})[2{G_{23}}^{fb}G^{mx} + ({G_{23}}^{fb} + G^{mx}){K_{23}}^{fb}](G^{mx} - K^{mx}) \quad (26)$$

$$b_2 = -2a_2 \quad (27)$$

$$b_3 = -2a_3 \quad (28)$$

$$b_4 = -4(G^{mx})^3({G_{23}}^{fb} - G^{mx})[{K_{23}}^{fb}G^{mx}K^{mx} - {G_{23}}^{fb}\{2G^{mx}({K_{23}}^{fb} - K^{mx}) + {K_{23}}^{fb}K^{mx}\}] \quad (29)$$

$$c_1 = 8(G^{mx}K^{mx})^2({G_{23}}^{fb} - G^{mx})[2{G_{23}}^{fb}G^{mx} + {K_{23}}^{fb}({G_{23}}^{fb} + G^{mx})] \quad (30)$$

$$c_2 = a_2 \quad (31)$$

$$c_3 = a_3 \quad (32)$$

$$c_4 = -2(G^{mx})^2K^{mx}({G_{23}}^{fb} - G^{mx})[{K_{23}}^{fb}G^{mx}K^{mx} - {G_{23}}^{fb}\{2G^{mx}({K_{23}}^{fb} - K^{mx}) + {K_{23}}^{fb}K^{mx}\}] \quad (33)$$

Thus, with 1% nano-clay, the elastic features of the banana-carbon fiber-reinforced nano-clay epoxy composite can be evaluated using Eqs. (12)-(16):

$E_1 = 119703.74MPa$

Where:

${K_{23}}^{CF} = \frac{E}{3(1-2\mu)} = \frac{15000}{3(1-2\times0.07)} = 5814MPa$; Similarly, ${K_{23}}^{BF} = 2636.4MPa$,

${K_{23}}^{NC} = 117333.3MPa, {K_{23}}^{IP} = 12888.9MPa, {K_{23}}^{mx} = 38888.9MPa$

$\upsilon_{12} = 0.27; G_{12} = 8510.27MPa + G_{NCP,12} = 6.92 \times 10^6 MPa$

$G_{23} = 65040650.2MPa + G_{NCP,23} = 7.2 \times 10^6 MPa$

Where: A, B, and C are calculated using Eqs. (17)-(19) and are given below:

$A = -1.23 \times 10^{28}; B = -2.5 \times 10^{32}; C = -1.44 \times 10^{28}$

Where:

$a_0 = -2.43 \times 10^{28}, a_1 = 5.32 \times 10^{28}, a_2 = -7.35 \times 10^{28}, a_3 = 2.98 \times 10^{28}, a_4 = 2.89 \times 10^{27}$
$b_0 = 6 \times 10^{27}, b_1 = -4.5 \times 10^{28}, b_2 = 14.7 \times 10^{28}, b_3 = -5.96 \times 10^{28}, b_4 = -5.2 \times 10^{33}$
$c_0 = 1, c_1 = 4.9 \times 10^{28}, c_2 = -7.35 \times 10^{28}, c_3 = 2.98 \times 10^{28}, c_4 = -4.9 \times 10^{26}$ (Values calculated using Eqs. (20)-(33))

Likewise, similar elastic properties of the proposed composite are evaluated for 3% and 5% nano-clay and are given in Table 4.

3.1.3. Bridging Model

The bridging micromechanical model (BM) was evolved by [51, 52] to determine the strength and rigidity of unidirectional composites. An easy version of this model was also developed [53] that gave closer results when compared to experimentally obtained values. The elastic features of the composite based on the bridging model are as follows [54]:

$$E_1 = {E_1}^{CF}V^{CF} + {E_1}^{BF}V^{BF} + E^{mx}V^{mx} + E^{NC}V^{NC} + E^{IP}V^{IP} \quad (34)$$

$$v_{12} = {v_{12}}^{CF} V^{CF} + {v_{12}}^{BF} V^{BF} + v^{mx} V^{mx} + v^{NC} V^{NC} + v^{IP} V^{IP} \tag{35}$$

$$E_2 = \frac{(V^{CF} + V^{mx} a_{11})(V^{CF} + V^{mx} a_{22})}{(V^{CF} + V^{mx} a_{11})({V^{CF}}{S_{22}}^{CF} + a_{22} V^{mx} {S_{22}}^{mx}) + V^{CF} V^{mx} ({S_{21}}^{mx} - {S_{21}}^{CF}) a_{12}} \tag{36}$$

Where:

$$S_{22} = \frac{1}{E_2}, S_{21} = \frac{-v_{21}}{E_2}, S_{23} = \frac{-v_{32}}{E_3} \tag{37}$$

$$a_{11} = \frac{E^{mx}}{{E_1}^{CF}}, a_{22} = a_{33} = a_{44} = 0.3 + 0.7\left(\frac{E^{mx}}{{E_2}^{CF}}\right), a_{12} = \left(\frac{{E_1}^{CF} v^{mx} - E^{mx} {v_{12}}^{CF}}{{E_1}^{CF} - E^{mx}}\right)(a_{11} - a_{22}) \tag{38}$$

$$G_{12} = \frac{(V^{CF} + V^{mx} a_{66}) {G_{12}}^{CF} G^{mx}}{V^{CF} G^{mx} + V^{mx} a_{66} {G_{12}}^{CF}} \tag{39}$$

$$G_{23} = \frac{0.5(V^{CF} + V^{mx} a_{44})}{V^{CF}({S_{22}}^{CF} - {S_{23}}^{CF}) + V^{mx} a_{44} ({S_{22}}^{mx} - {S_{23}}^{mx})} \tag{40}$$

$$a_{66} = 0.3 + 0.7\left(\frac{G^{mx}}{{G_{12}}^{CF}}\right) \tag{41}$$

Thus for 1% nano-clay, the elastic features of the banana-carbon fiber-reinforced nano-clay epoxy composite can be evaluated using equations (34)-(36):

$E_1 = 119670.47MPa; v_{12} = 0.26$

$E_2 = 20609.87MPa$
$\because a_{11} = 0.152, a_{22} = 1.933, a_{12} = -0.6713, {S_{22}}^{CF} = 6.67 \times 10^{-5}, {S_{22}}^{mx} = 2.86 \times 10^{-5},$
${S_{21}}^{mx} = -1 \times 10^{-5}, {S_{21}}^{CF} = -8.69 \times 10^{-7}$
$= 20609.87MPa + E_{NCP,22}$
$= 1.7342 \times 10^{13} MPa$

$G_{12} = 8645.6MPa$
$\because a_{66} = 0.45$
$= 8645.6MPa + G_{NCP,12}$
$= 6.93 \times 10^{6} MPa$
$G_{23} = 9262.83MPa$
$\because a_{44} = a_{22} = 1.933, {S_{22}}^{CF} = 6.67 \times 10^{-5}, {S_{23}}^{CF} = -4.67 \times 10^{-6}, {S_{23}}^{mx}$
$= -1 \times 10^{-5}, {S_{22}}^{mx} = 2.86 \times 10^{-5}$
$= 9262.83MPa + G_{NCP,23}$
$= 6.93 \times 10^{6} MPa$

Likewise, similar elastic properties of the proposed composite are evaluated for 3% and 5% nano-clay and are given in Table 4.

3.2. Semi-Empirical Model

Semi-empirical models also known as semi-physical models are found to rely on parameters having natural significance [55, 56]. Semi-empirical relations have corrected or fitting parameters that make design procedures simple and easy [57, 58].A semi-empirical micromechanical model, also known as the modified Halpin-Tsai (Mod. H-T)

model is developed by exhibiting the matrix modulus in terms of fiber diameter and by establishing an equivalent constant. This model helps in deciding the threshold weight and volume fraction of the inclusion so that the matrix modulus can be maintained more the needed level [56].

3.2.1. Modified Halpin-Tsai

This semi-empirical model was developed by Halpin-Tsai (Modified Halpin-Tsai) to rectify the Young's modulus in transverse direction as obtained by the rule of mixture method (ROM). A modified Halpin-Tsai method based on finite elemental research was suggested, considering the possibility of a numerous fiber arrangements [59]. The transverse Young's modulus and in-plane modulus of rigidity as proposed by [60] are given by:

$$E_2 = E^{mx}\left(\frac{1+\xi_{E_2}\eta_{E_2}V^{CF}}{1-\xi_{E_2}V^{CF}}\right) \tag{42}$$

$$G_{12} = G^{mx}\left(\frac{1+\xi_{G_{12}}\eta_{G_{12}}V^{CF}}{1-\eta G_{12}V^{CF}}\right) \tag{43}$$

Where, $V^{CF} < 0.3$

$$\eta_{E_2} = \frac{\left(\frac{E_2{}^{CF}}{E^{mx}}\right)-1}{\left(\frac{E_2{}^{CF}}{E^{mx}}\right)+\xi_{E_2}}; \quad \xi_{E_2} = \{4.924 - 35.888V^{CF} + 125.118V^{CF^2} - 145.121V^{CF^3}\} \quad \text{if}$$

$V_{CF} \geq 0.3$; $\xi_{E_2} = \{1.5 + 5500V^{CF^{18}}$ if $V_{CF} \geq 0.3$

$$\eta_{G_{12}} = \frac{\left(\frac{G_{12}{}^{CF}}{G^{mx}}\right)-1}{\left(\frac{G_{12}{}^{CF}}{G^{mx}}\right)+\xi_{G_{12}}}; \xi_{G_{12}} = 1 + 40V^{CF^{10}}$$

The longitudinal elastic modulus and in-plane Poisson's ratio will be the same as that in ROM.

$$E_1 = E_1{}^{CF}V^{CF} + E_1{}^{BF}V^{BF} + E^{mx}V^{mx} + E^{NC}V^{NC} + E^{IP}V^{IP} \tag{44}$$

$$\upsilon_{12} = \upsilon_{12}{}^{CF}V^{CF} + \upsilon_{12}{}^{BF}V^{BF} + \upsilon^{mx}V^{mx} + \upsilon^{NC}V^{NC} + \upsilon^{IP}V^{IP} \tag{45}$$

Thus for 1% nano-clay, the elastic features of the banana-carbon fiber-reinforced nano-clay epoxy composite can be evaluated using Eqs. (42)-(43) and Eqs. (44)-(45):

$$\eta_{E_2} = \frac{\left(\frac{15}{35}\right)-1}{\left(\frac{15}{35}\right)+1.5} = -1.1$$

$\because \xi_{E_2} = 1.5 + 5500 \times 0.47^{18} = 1.5 (V^{CF} = 0.47)$

$\therefore E_2 = 5179.63MPa + E_{NCP,22}$

$= 1.7342 \times 10^{13} MPa$

$$\eta_{G_{12}} = \frac{\left(\frac{15000}{3200}\right)-1}{\left(\frac{15000}{3200}\right)+1.02} = 0.65$$

$\because \xi_{G_{12}} = 1 + 40 \times 0.47^{10} = 1.02 (V^{CF} = 0.47)$

$\therefore G_{12} = 6034.13MPa + G_{NCP,12}$
$= 6.94 \times 10^6 MPa$

$E_1 = 119670.47MPa$
$\upsilon_{12} = 0.26$

Likewise, similar elastic properties of the proposed composite are evaluated for 3% and 5% nano-clay and are given in Table 4.

3.3. Calculation of Elastic Properties for Nano-Clay Platelets

In an intercalated banana-carbon fiber-reinforced nano-clay epoxy composite, the nano-clay platelet is surrounded by a layer of interphase at the top surface, and epoxy is used as a binding medium. The relation between the thickness of silicate layer (t_{SL}), number of silicate sheets (N), and the interlayer gap between nano-clay plateletsd_{gap} in composites are as follows [61].

$$t = (N-1)d_{gap} + t_{SL} \tag{46}$$

The following formulae wereproposed as per modified ROM for calculating elastic properties of nano-clay platelets (consisting of nano-clay and interphase) [62].

$$E_{NCP,11} = E_{NCP,33} = \chi_{NC}E_{NC} + \chi_{IP}E_{IP} \tag{47}$$

$$E_{NCP,22} = \frac{E_{NC}E_{IP}}{\chi_{NC}E_{IP} + \chi_{IP}E_{NC} - \chi_{NC}\chi_{IP}\beta E_{NC}E_{IP}} \tag{48}$$

$$\upsilon_{NCP,12} = \upsilon_{NCP,32} = \chi_{NC}\upsilon_{IP} + \chi_{IP}\upsilon_{NC} \tag{49}$$

$$\upsilon_{NCP,13} = \frac{\chi_{NC}\upsilon_{NC}E_{NC}(1-\upsilon_{IP}{}^2) + \chi_{IP}\upsilon_{IP}E_{IP}(1-\upsilon_{NC}{}^2)}{\chi_{NC}E_{NC}(1-\upsilon_{IP}{}^2) + \chi_{IP}\upsilon_{IP}E_{IP}(1-\upsilon_{NC}{}^2)} \tag{50}$$

$$G_{NCP,12} = G_{NCP,32} = \frac{G_{NC}G_{IP}}{\chi_{NC}G_{IP} + \chi_{IP}G_{NC} - \chi_{NC}\chi_{IP}\eta G_{NC}G_{IP}} \tag{51}$$

$$G_{NCP,13} = \frac{E_{NCP,11}}{2(1+\upsilon_{NCP,13})} \tag{52}$$

Where:

$$\beta = \frac{\upsilon_{NC}{}^2\frac{E_{IP}}{E_{NC}} + \upsilon_{IP}{}^2\frac{E_{NC}}{E_{IP}} - 2\upsilon_{NC}\upsilon_{IP}}{\chi_{NC}E_{NC} + \chi_{IP}E_{IP}}$$

$$\eta = \frac{\upsilon_{NC}{}^2\frac{G_{IP}}{G_{NC}} + \upsilon_{IP}{}^2\frac{G_{NC}}{G_{IP}} - -2\upsilon_{NC}\upsilon_{IP}}{\chi_{NC}G_{NC} + \chi_{IP}G_{IP}}$$

For 1% nano-clay:

$E_{NCP,22} = 1734.22 \times 10^{10} MPa$

Where $\beta = 6.49 \times 10^{-4}$
$G_{NCP,12} = G_{NCP,23} = 6.92 \times 10^6 MPa$

Where:

$\eta = 1.65 \times 10^{-3}$
$\upsilon_{NCP,13} = 0.27$

4. Finite Element Work

4.1. Model Configuration

The composite sampleis modeledand examined for its mechanical properties on ANSYS Mechanical APDL software. The sample measurements used in this examination are as per ASTM D3039 standards [42]: length of the sample = 30 mm, width of the sample = 200 mm and thickness of lamina = 0.5mm/layer. Number of sheets = 5.

The total depth of the samples = 2.5mm, Degree of Freedom = zero,

Both sides of the samples are constrained. After modeling the sample, it is meshed using a mesh tool. Number of mesh: Number of vertical element divisions = 20; Number of horizontal element division=15. Meshed model is shown in Fig. 1.

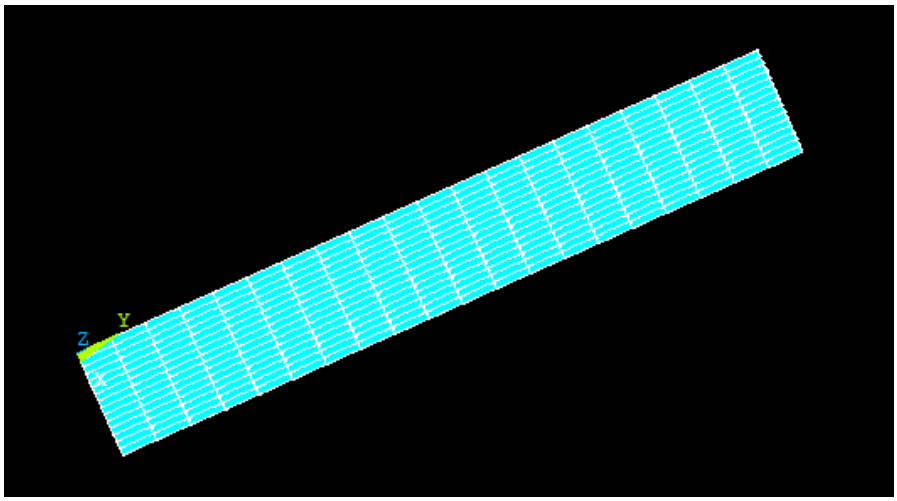

Fig. 1 Meshed model

4.2 Loads and Orientation of the Fibers

The examination of the properties is carried out by using element 3D 4 Shell 181. A point load of 200KN [42] is applied to the model at 21 nodes in a perpendicular direction (along -z axis) as shown in (Fig. 4). The sample is configured in the sequence of layers: banana fiber - carbon fiber - nano-clay platelet - carbon fiber - banana fiber at orientation angles of 90°, 0°, 90°,0°, and 90° respectively also portrayed in Fig. 2. The modeled layers in ANSYS APDL are shown in Fig. 3. The vector sum distortion for the proposed composite material is analysed for the proposed composite reinforced with 1%, 3%, and 5% nano-clay particles and is given in Table 4. The vector sum deformation plots developed by using the ANSYS APDL application for NC composition of 1%, 3% & 5% are also shown in Fig. 5.

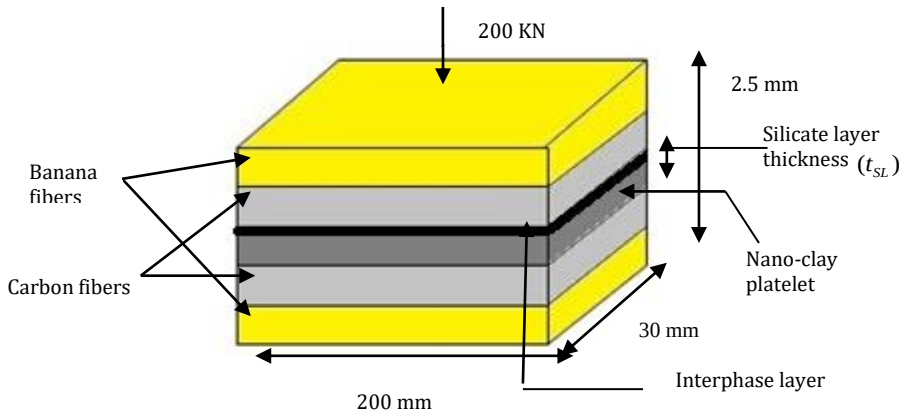

Fig. 2 Application of load on arrangement of fibers and nano-clay platelet.

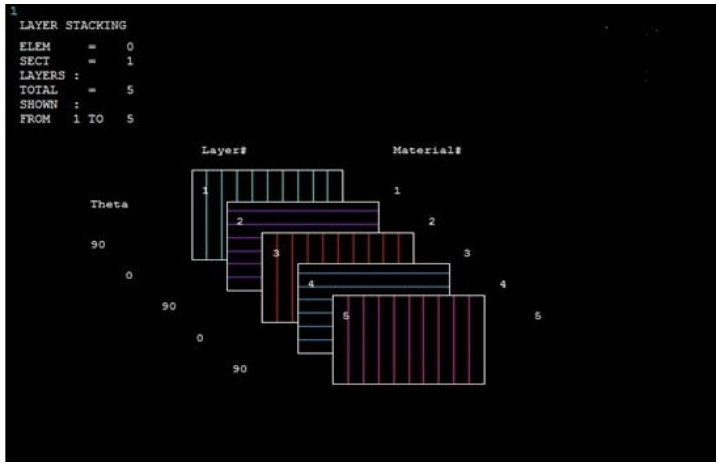

Fig. 3 Modelled layers in ANSYS APDL

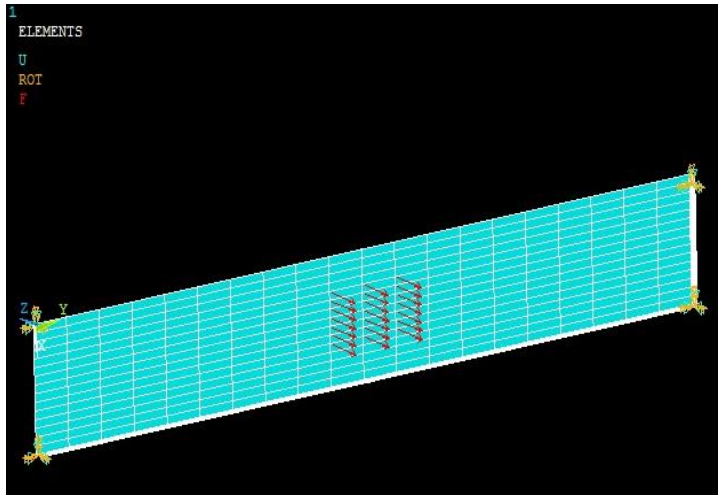

Fig. 4 FE model showing point load at 21 nodes (along -z axis)

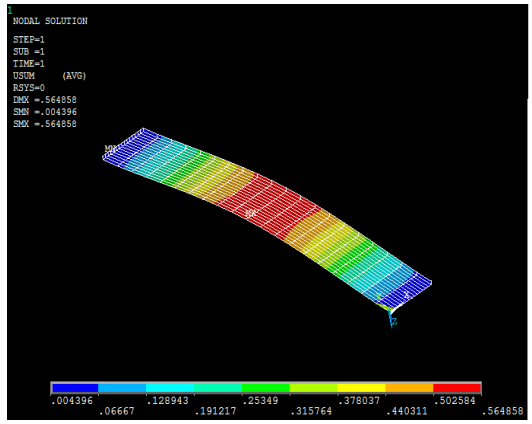

(a)

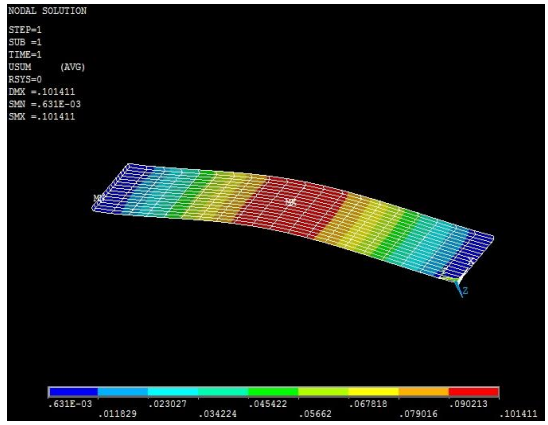

(b)

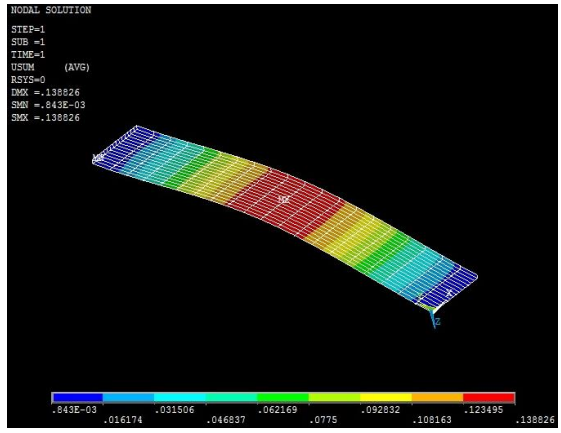

(c)

Fig. 5 Vector sum deformation for banana-carbon fiber reinforced nano-clay epoxy composite having (a) 1 percent, (b) 3 percent and (c) 5 percent nano-clay.

Table 4. Elastic properties, vector sum deformation and FE model results for different percentages of NC filler in the proposed composite

Nano-clay %	Elastic Properties	Mori-Tanaka Model	Generalized Self-Consistent Model	Bridging Model	Modified Halpin-Tsai Model	Vector sum deformation from ANSYS(mm)	FE model
1%	E_1 (MPa)	119797.9	119703.74	119670.47	119670.47	0.56485	116223.71
	υ_{12}	0.24	0.27	0.26	0.26		0.28
	E_2 (MPa)	1.7100×10^{13}	**	1.7342×10^{13}	1.7342×10^{13}		1.6602×10^{13}
	G_{12} (MPa)	6.93×10^{6}	6.92×10^{6}	6.93×10^{6}	6.94×10^{6}		6.66×10^{6}
	G_{23} (MPa)	6.93×10^{6}	7.2×10^{6}	6.93×10^{6}	**		6.66×10^{6}
3%	E_1 (MPa)	122278.9	113792.3	122160	122160	0.10141	117575.8
	υ_{12}	0.24	0.27	0.27	0.26		0.28
	E_2 (MPa)	3.86×10^{5}	**	3.97×10^{5}	392467.5		3.67×10^{5}
	G_{12} (MPa)	7.02×10^{6}	7.02×10^{6}	7.02×10^{6}	7.03×10^{6}		6.75×10^{6}
	G_{23} (MPa)	7.02×10^{6}	6.12×10^{6}	7.02×10^{6}	**		6.75×10^{6}
5%	E_1 (MPa)	126742.3	130573.9	126614.8	126614.8	0.13883	123050.7
	υ_{12}	0.25	0.26	0.26	0.26		0.27
	E_2 (MPa)	412231.3	**	402651.4	432231.2		396376.2
	G_{12} (MPa)	8.11×10^{6}	8.11×10^{6}	8.11×10^{6}	8.20×10^{6}		7.87×10^{6}
	G_{23} (MPa)	8.11×10^{6}	7.09×10^{6}	8.11×10^{6}	**		7.87×10^{6}

5. Fiber Hybridization and Its Effect

The hybridization of fiber is a technique for improving the composite properties [63, 64]. The study of hybrid effect is significant in the analysis of the property of the proposed composite. The hybridization is important in understanding the behavior of the fibers in the hybrid composite. It, in general, predicts that the failure strain of a hybrid composite differs from the composites blended with either of the parent fibers alone. Fiber-hybrid composites are composed of high and low elongation fibers. In this study, high and low elongation fibers are banana and carbon fiber respectively. The outcome of placing a carbon fiber sheet in between glass fiber sheets was first reported by [65]. Carbon fiber layers failed in tension. The strain (ε_c) was noted to be increased by 40% (ε_c'). This increase is termed as the 'hybrid effect', that is normally expected for failure strain [65]. The hybrid effect (Eq. (53)) is the ratio of the failure strain of the hybrid composite to the failure strain of the low elongation fiber-blended composite [66].

$$\text{Hybridization effect} = \frac{\varepsilon_c' - \varepsilon_c}{\varepsilon_c} \tag{53}$$

Where ε_c'=increased tensile strain of the hybrid compositeat breaking point.

ε_c = tensile strain of the carbon fiber at breaking point.

The hybrid effect R_{hyb} as given by [66] is:

$$R_{hyb} = \frac{\bar{\varepsilon}_{HEC}}{\bar{\varepsilon}_{LEC}} = \sqrt{\frac{\bar{\varepsilon}_{HEF}}{\bar{\varepsilon}_{LEF}}} \left[\frac{\delta_h (k_h{}^q - 1)}{2\delta (k^q - 1)} \right]^{\frac{-1}{2m}} \tag{54}$$

Where $\bar{\varepsilon}_{LEF}$= mean strain of the least elongated fiber at breaking point.

$\bar{\varepsilon}_{LEF}$= mean strain of the highest elongated fiber at breaking point.

q= Wei bulls shape parameter.

$$R_{hyb} = \left[\frac{\delta_h (k_h{}^q - 1)}{2\delta (k^q - 1)} \right]^{\frac{-1}{2q}} \tag{55}$$

The ineffective length $\delta$and $\delta_{\square}$ for the hybrid composite is given by [66]:

$$\delta = 1.531 \left(\frac{E_1 A_1 d}{gh} \right)^{1/2} \tag{56}$$

$$\delta_h = \frac{2}{\rho^{1/2}} \left(\frac{E_1 A_1 d}{Gh} \right)^{1/2} \frac{m_2{}^2 - m_1{}^2}{m_1 (2 - m_1{}^2) - m_2 (2 - m_2{}^2)} \tag{57}$$

Where: the ratio of fibers' extensional stiffness(ρ) is given by [66]:

$$\rho = \frac{E_1 A_1}{E_2 A_2}$$

$$\rho = \frac{3.48}{230} = 0.015$$

Where:

$E_1 A_1$ =Denotative stiffness of LE fibers.

$E_2 A_2$ =Denotative stiffness of HE fibers.

h= Matrix depth.

d= Fiber spacing.

G= Shear matrix modulus.

The strain and strain concentration parameters K and K_h respectively and a constant $m_{1,2}$ are given by [66]:

$K = 1.293$

$$K_h = 1 + \frac{m_2 - m_1}{m_1 (2 - m_1{}^2) - m_2 (2 - m_2{}^2)} \tag{58}$$

$$m_{1,2} = \left(\frac{\rho + 1 \pm (\rho^2 + 1)^{\frac{1}{2}}}{\rho} \right)^{\frac{1}{2}} \tag{59}$$

Substituting the value of ρobtained above in Eq. (59), we get:

$m_1 = 11.5$ and $m_2 = 1.0$.

Substituting the values of $m_2 \& m_2$ obtained above in Eq. (58), we get:

$$K_h = 1.007 \approx 1.01$$

$\delta \& \delta_h$ are calculated using Eqs. (56) and (57) as:

$$\delta = 1.531\left(\frac{230 \times 10^3 \times (200 \times 30) \times 30}{3200 \times 1 \times 1000^2}\right)^{\frac{1}{2}} = 5.5$$

$$\delta_h = \frac{2}{\sqrt{0.015}}(3.6)\left(\frac{1.0^2 - 11.5^2}{11.5(2-11.5^2) - 1.0(2-1.0^2)}\right) = 5.15$$

$$\therefore R_{hyb} = \left[\frac{5.15(1.01^5 - 1)}{2 \times 5.5(1.293^5 - 1)}\right]^{-1/2\times 5} ; q \approx 5$$

$$= \frac{0.263}{28.75} = 1.6$$

The tensile failure strain of the banana-carbon fiber blended epoxy composite is 1.6 times more than the composites fabricated from carbon fibers alone.

6. Results and Discussion

In this study, the proposed composite reinforced with 1%, 3%, and 5% nano-clay particles is modeled in ANSYS APDL and various analytical equations are employed to find its effective elastic features. The main purpose is to analyze the comparison among the different elastic properties obtained using homogenization and semi-empirical models, to calculate the average error and deformation for 1%, 3%, and 5% nano-clay reinforcements. The average error (E_{AV}) is calculated using the following equation [70]:

$$E_{AV} = \left|\frac{x_c - x_m}{x_m}\right| \times 100 \quad (60)$$

Where: x_c = Elastic values obtained by calculations

x_m = elastic values obtained by Finite element results

The average value of the tensile modulus obtained by different analytical models for the proposed composite blended with 1 wt% of nano-clay (with interphase) shows an increase of 88.35% on comparing it to the value of tensile modulus of 13950MPa for carbon fibers reinforced with 1 wt% of nano-clay filled IPN matrix [9]. For 3 wt% of nano-clay (with interphase), the average tensile modulus shows a rise of 88.1%, as compared to the tensile modulus value of 14550MPa [9]. From the results, it is observed that the inclusion of banana fibers increases the strength and toughness of nano-clay reinforced banana-carbon fibers composites.

The inclusion of 5 wt% of NC (with interphase) to the proposed composite shows an increase of 66 % on comparing it to the value of tensile modulus of 43000MPa obtained for NaOH treated banana fiber composite infused with 6 wt% of NC [7]. Therefore the results of FE model obtained for the proposed composite is validated with the analytical models used in this study and with experiments in literatures [7] and [9].

For 1%, 3% and 5% reinforcements of NC fillers, the average error values are evaluated for all the analytical models and for different elastic properties and are presented in Fig. 6. These errors show the percent deviation from the elastic values obtained from FEM results. The following points are highlighted from the results presented in Fig. 6(a) and 6 (b) for longitudinal elastic modulus(E_1) and in-plane Poisson's ratio (υ_{12}):

6.1. Longitudinal elastic modulus(E_1)

It can be observed from Fig. 6(a), that for 1% NC, all the models are in good concurrence with the FEM results as all the models are showing low average errors. For 3% NC reinforcement, the Mori-Tanaka model is yielding the largest variation from FEM value and for 5% NC, the Mori-Tanaka model gives the least percent error among all the other models used. It is evident from Fig. 6(a), that all the models for 1% NC are showing the best agreement with FEM results as compared to the error percent of all the models for 3% and 5% NC reinforcements. From the elastic values obtained for E_1, it is found that among 1%, 3% and 5% reinforcements, the proposed composite reinforced with 5% NC gives the stiffer composite

In-plane Poisson's ratio. (υ_{12}): It can be observed from Fig. 6(b), that for 1% NC, only Generalized-Self Consistent model is showing good concurrence with FEM result. For 3% NC, both Generalized-Self Consistent model and Bridging model are yielding less variations from FEM values as compared to Mori-Tanaka and Modified Halpin-Tsai models. For 5% NC, the Mori-Tanaka model is showing the highest percent error. It is clear from Fig. 6(b) that all the models for 5% NC reinforcement, are showing the best agreement with FEM results as compared to error percent obtained for 1%, 3% and 5% NC.

The highlights for the result presented in Fig. 6(c) for transverse elastic modulusE_2 are

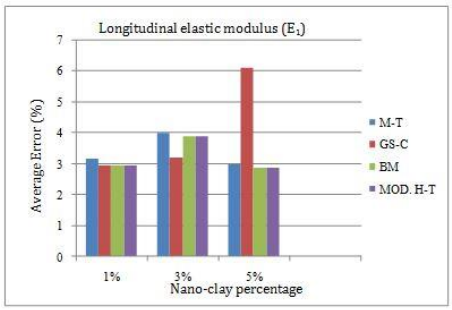

(a)

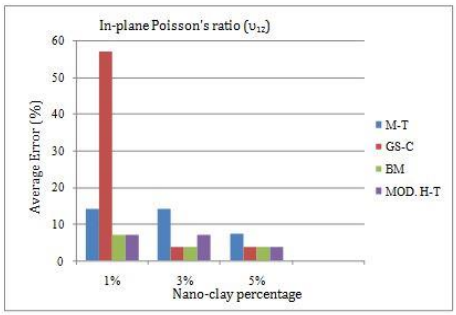

(b)

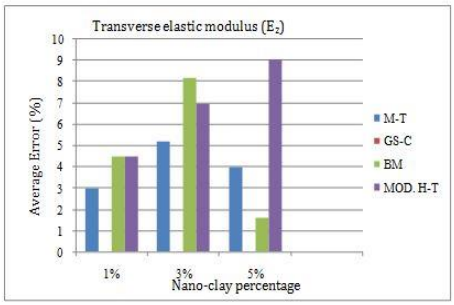

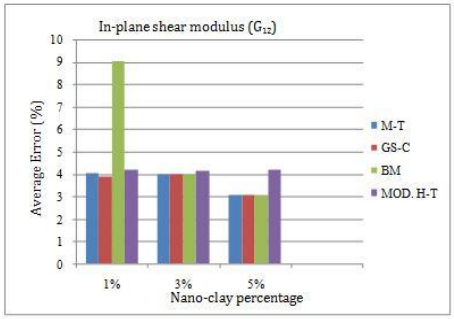

(c) (d)

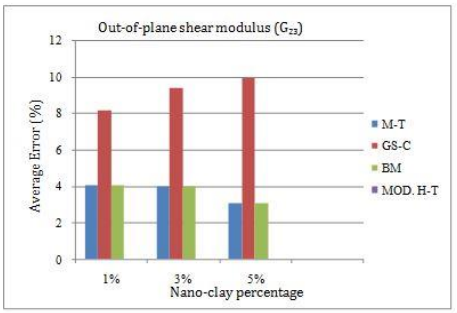

(e)

Fig. 6 Results for the average error for (a) Longitudinal elastic modulus (b) In-plane Poisson's ratio (c) Transverse elastic modulus (d) In-plane shear modulus (e) Out-of-plane shear modulus

6.2. Transverse elastic modulus(E_2)

From Fig. 6(c), it is clear that for 1% NC filler, all the models are showing good concurrence with the FEM results. For 3% NC, all the models are yielding high variations and for 5% NC, the Bridging model outperforms all the other models as it is showing the least percent error. It is evident from Fig. 6(c) that all the models for 1% NC are showing the best agreement with FEM results as compared to the error percent obtained for 3% and 5% NC reinforcements. From the elastic values obtained for E_2, it can be deduced that the proposed composite reinforced with 1% NC is stronger in the transverse direction as compared to 3% and 5% NC reinforcements.

The main highlights for the results of in-plane shear modulus (G_{12}) and out-of-plane shear modulus (G_{23}), presented in Fig. 6(d) and 6(e) respectively are:

6.3. In-plane shear modulus (G_{12})

From Fig. 6(d), it is clear that all the models are showing good agreement with FEM results except the Bridging model for 1% NC reinforcement. It indicates that the NC reinforcement percentage does not have a significant influence on this property.

Out-of-plane shear modulus (G_{23}): All the models for 1%, 3% and 5% NC fillers are yielding low percent errors, as it can be observed from Fig. 6(e), except the Generalized-Self Consistent model is showing very high deviation from FEM results.

For the values of vector sum deformation given in Table 4, the following is observed:

6.4. Vector sum deformation

Banana and carbon-reinforced nano-clay epoxy composite for 3% nano-clay reinforcement is found the most suitable and for 1% nano-clay, the least suitable in terms of strength and deformation resistance as it is showing the lowest and highest total sum deformation respectively.

7. Conclusions

A novel composite material banana-carbon fiber-reinforced nano-clay epoxy composite is developed. The proposed composite is analyzed by using analytical models, namely Mori-

Tanaka, Bridging, Generalized Self-Consistent, and Modified Halpin-Tsai model for the calculation of elastic properties like longitudinal and transverse elastic modulus, in-plane and out-of-plane shear modulus, and in-plane Poisson's ratio. The average error is calculated for all the elastic properties obtained from different models for 1%, 3%, and 5% nano-clay reinforcements. From the results of this study, the following points are deduced:

- The modified Halpin-Tsai method is yielding the most effective elastic properties for the proposed composite as it gives the lowest average error percent on comparing with FEM results, and the Mori-Tanaka model is giving the least effective results.
- The composite reinforced with 5% NC is stiffest, as it yields the higher values of longitudinal elastic modulus than the corresponding values obtained for 1% and 3% NC reinforcements.
- For different weight percentages of NC reinforcements, GS-C model is yielding the best elastic properties for 5% NC as compared to all the other models used in the study.
- On arranging fibers in the sequence of banana at 90°, carbon at 0°, nano-clay at 90°, carbon at 0°, and banana at 90°, the total sum deformation for 3% nano-clay composition is found to be least, so it can be deduced that the proposed composite reinforced with 3% NC can sustain the maximum load and is of higher strength as compared to the composite blended with 1% and 5% NC. The composite reinforced with 1% NC reinforcement is weakest in terms of strength as it gives the highest deformation.
- The value of hybridization obtained for the proposed composite is 1.6. It depicts that banana fiber (HE fiber) in the hybrid composite is 1.6 times stiffer than carbon fiber (LE fiber) in the hybrid composite. It is found that the inclusion of banana fiber in the carbon fiber reinforced composites improves the failure strain rate of the hybrid composite. The hybrid composite becomes much stronger in terms of strength as the tensile failure strain characteristics increases in comparison to the failure strain of carbon fiber (LE fiber) blended non-hybrid composite.

Abbreviations

$V_{fb/mx/NC}$	The volume fraction of fiber, matrix, and nano-clay.
$W_{fb/mx/NC}$	The weight percentage of fiber, matrix, and nano-clay.
$\rho_{fb/mx/NC}$	The density of fiber, matrix, and nano-clay.
ρ_C	The density of composite.
$W_{CF}/W_{BF}/W_{EP}/W_{NC}$	The weight percentage of carbon fiber, banana fiber, epoxy, and nano-clay respectively.
$\rho_{CF}/\rho_{BF}/\rho_{EP}/\rho_{NC}$	The density of carbon fiber, banana fiber, epoxy, and nano-clay respectively.
$V_{CF}/V_{BF}/V_{EP}/V_{NC}/V_{IP}$	The volume fraction of carbon fiber, banana fiber, epoxy and nano-clay, and interphase.
E_{NC}/E_{IP}	Elastic modulus of nano-clay and interphase

	respectively.
G_{NC}/G_{IP}	Shear modulus of nano-clay and interphase respectively.
$\upsilon_{NC}/\upsilon_{IP}$	Poisson's ratio of nano-clay and interphase respectively.
${E_1}^{fb/mx}$	Elastic modulus of fiber and matrix in longitudinal direction.
${E_{22}}^{fb} = {E_{33}}^{fb}$	Elastic modulus of fiber and matrix in transverse direction.
${G_{12}}^{fb/mx} = {G_{13}}^{fb/mx}$	In-plane shear modulus of fiber, matrix.
${G_{23}}^{fb}$	Out-of-plane shear modulus of fiber.
${\upsilon_{12}}^{fb/mx} = {\upsilon_{31}}^{fb/mx}$	In-plane Poisson's ratio of fiber, matrix.
${\upsilon_{23}}^{fb}$	Out-of-plane Poisson's ratio of fiber.
$\rho^{fb/mx}$	The density of fiber, matrix.
${K_{23}}^{fb/mx}$	Strain bulk modulus of fiber, matrix.
${K_{23}}^{CF}/{K_{23}}^{BF}$	Strain bulk modulus of fiber, matrix.
K_{23}	Plain strain bulk modulus.
a_{ij}	Coefficients of bridging matrix A [40, 41].
${S_{21}}^{CF}/{S_{22}}^{CF}$	Coefficients of the compliance matrix of carbon fiber.
${S_{21}}^{mx}/{S_{21}}^{mx}$	Coefficients of the compliance matrix of the epoxy matrix.
η_{E_2} $\eta_{G_{12}}$ ξ_{E_2} $\xi_{G_{12}}$	Dimensionless parameters.
E_1	Elastic modulus of the composite in longitudinal direction.
E_2	Elastic modulus of the composite in transverse direction.
υ_{12}	In-plane Poisson's ratio of the composite.
G_{12}	In-plane shear modulus of the composite.
G_{23}	Out-of-plane shear modulus of the composite.

$E_{NCP,11} = E_{NCP,33}$	Longitudinal elastic modulus of nano-clay platelet.
$E_{NCP,22}$	Transverse elastic modulus of nano-clay platelet.
$G_{NCP,12} = G_{NCP,32}$	In-plane shear modulus of nano-clay platelet.
$G_{NCP,13}$	Out-of-plane shear modulus of nano-clay platelet.
$\upsilon_{NCP,12} = \upsilon_{NCP,32}$	In-pane Poisson's ratio of nano-clay platelet.
$\upsilon_{NCP,13}$	Out-of-plane Poisson's ratio of nano-clay platelet/
χ_{NC}	Volume fraction of nano-clay.
χ_{IP}	Volume fraction of interphase.
t_{SL}	Thickness of silicate layer.
d_{gap}	Interlayer gap between nano-clay platelets.
N	Number of silicate sheets.

Acknowledgment

The author would like to express deep thanks to the editorial team and anonymous reviewers for their positive comments for previous version of this research paper.

References

[1] Saxena T, Tomar P. Constitutive Performance Characterization of Diversified Bamboo Material-A Green Technology. Proceedings of International Conference on Sustainable Computing in Science, Technology and Management (SUSCOM), Amity University Rajasthan, Jaipur-India, Feb, 2008.

[2] Parashar S, Tomar P. Synergy of sustainable bio-composite bamboo material in green technology-an explicit report. Proceedings of International Conference on Sustainable Computing in Science, Technology and Management (SUSCOM), Amity University Rajasthan, Jaipur-India, Feb, 2008.

[3] Saxena T, Chawla VK. Effect of fiber orientations and their weight percentage on banana fiber-based hybrid composite. Materials Today: Proceedings. 2022;50:1275-81. https://doi.org/10.1016/j.matpr.2021.08.149

[4] Saba N, Jawaid M, Asim M. Recent advances in nanoclay/natural fibers hybrid composites. Nanoclay reinforced polymer composites. 2016:1-28. https://doi.org/10.1007/978-981-10-0950-1_1

[5] Kumar A, Angra S, Chanda AK. Analysis of the effects of varying core thicknesses of Kevlar Honeycomb sandwich structures under different regimes of testing. Materials Today: Proceedings. 2020;21:1615-23. https://doi.org/10.1016/j.matpr.2019.11.242

[6] Usuki A, Kojima Y, Kawasumi M, Okada A, Fukushima Y, Kurauchi T, Kamigaito O. Synthesis of nylon 6-clay hybrid. Journal of Materials Research. 1993;8(5):1179-84. https://doi.org/10.1557/JMR.1993.1179

[7] Mohan TP, Kanny K. Nanoclay infused banana fiber and its effects on mechanical and thermal properties of composites. Journal of Composite Materials. 2016;50(9):1261-76. https://doi.org/10.1177/0021998315590265

[8] Mohan TP, Kanny K. Compressive characteristics of unmodified and nanoclay treated banana fiber reinforced epoxy composite cylinders. Composites Part B: Engineering. 2019;169:118-25. https://doi.org/10.1016/j.compositesb.2019.03.071
[9] Suresh G, Vivek S, Babu LG, Bernard SS, Akash RM, Kanna SR, Kumar SB, Sethuramalingam P. Evaluation of mechanical behaviour of carbon fiber reinforced nanoclay filled IPN matrix composite. Materials Research Express. 2019;6(12):125311. https://doi.org/10.1088/2053-1591/ab54ec
[10] Saxena T, Chawla VK. Banana leaf fiber-based green composite: An explicit review report. Materials Today: Proceedings. 2021;46:6618-24. https://doi.org/10.1016/j.matpr.2021.04.099
[11] Yang G, Wang C, Wen P, Yin W. Performance characteristics of cold-mixed porous friction course with composite-modified emulsified asphalt. Journal of Materials in Civil Engineering. 2020;32(3):04019372. https://doi.org/10.1061/(ASCE)MT.1943-5533.0003047
[12] Brune DA, Bicerano J. Micromechanics of nanocomposites: comparison of tensile and compressive elastic moduli, and prediction of effects of incomplete exfoliation and imperfect alignment on modulus. Polymer. 2002;43(2):369-87. https://doi.org/10.1016/S0032-3861(01)00543-2
[13] Kojima Y, Usuki A, Kawasumi M, Okada A, Fukushima Y, Kurauchi T, Kamigaito O. Mechanical properties of nylon 6-clay hybrid. Journal of Materials Research. 1993;8(5):1185-9.. https://doi.org/10.1557/JMR.1993.1185
[14] Ji XL, Jing JK, Jiang W, Jiang BZ. Tensile modulus of polymer nanocomposites. Polymer Engineering & Science. 2002;42(5):983-93. https://doi.org/10.1002/pen.11007
[15] Parashar S, Chawla VK. A systematic review on sustainable green fibre reinforced composite and their analytical models. Materials Today: Proceedings. 2021;46:6541-6. https://doi.org/10.1016/j.matpr.2021.03.739
[16] Parashar S, Chawla VK. Evaluation of fiber volume fraction of kenaf-coir-epoxy based green composite by finite element analysis. Materials Today: Proceedings. 2022;50:1265-74. https://doi.org/10.1016/j.matpr.2021.08.147
[17] Faghidian SA. Flexure mechanics of nonlocal modified gradient nano-beams. Journal of Computational Design and Engineering. 2021;8(3):949-59. https://doi.org/10.1093/jcde/qwab027
[18] Faghidian SA. Higher order mixture nonlocal gradient theory of wave propagation. Mathematical Methods in the Applied Sciences. 2020; Sep 18.. https://doi.org/10.1002/mma.6885
[19] Faghidian SA. Two-phase local/nonlocal gradient mechanics of elastic torsion. Mathematical Methods in the Applied Sciences. 2020 Sep 14. https://doi.org/10.1002/mma.6877
[20] Faghidian SA. Contribution of nonlocal integral elasticity to modified strain gradient theory. The European Physical Journal Plus. 2021;136(5):559. https://doi.org/10.1140/epjp/s13360-021-01520-x
[21] Kalaitzidou K, Fukushima H, Miyagawa H, Drzal LT. Flexural and tensile moduli of polypropylene nanocomposites and comparison of experimental data to Halpin-Tsai and Tandon-Weng models. Polymer Engineering & Science. 2007;47(11):1796-803. https://doi.org/10.1002/pen.20879
[22] Hbaieb K, Wang QX, Chia YH, Cotterell B. Modelling stiffness of polymer/clay nanocomposites. Polymer. 2007;48(3):901-9. https://doi.org/10.1016/j.polymer.2006.11.062
[23] Wang, H. W., Zhou, H. W., Peng, R. D., &MishnaevskyJr, L. (2011). Nanoreinforced polymer composites: 3D FEM modeling with effective interface concept. Composites Science and Technology, 71(7), 980-988. https://doi.org/10.1016/j.compscitech.2011.03.003

[24] MishnaevskyJr L. Micromechanical analysis of nanocomposites using 3D voxel based material model. Composites Science and Technology. 2012;72(10):1167-77. https://doi.org/10.1016/j.compscitech.2012.03.026
[25] Dai G, MishnaevskyJr L. Damage evolution in nanoclay-reinforced polymers: a three-dimensional computational study. Composites science and technology. 2013;74:67-77.. https://doi.org/10.1016/j.compscitech.2012.10.003
[26] Andrianov IV, Awrejcewicz J, Danishevskyy VV. Asymptotical mechanics of composites. Cham, Germany: Springer. doi. 2018;10:978-3.. https://doi.org/10.1007/978-3-319-65786-8
[27] Shah PD, Melo JD, Ciminijr CA, Ridha M. Evaluation of notched strength of composite laminates for structural design. Journal of composite materials. 2010;44(20):2381-92.. https://doi.org/10.1177/0021998310372713
[28] Tsai SW, Melo JD. An invariant-based theory of composites. Composites Science and Technology. 2014;100:237-43. https://doi.org/10.1016/j.compscitech.2014.06.017
[29] Xu W, Zeng Q, Yu A. Young's modulus of effective clay clusters in polymer nanocomposites. Polymer. 2012;53(17):3735-40. https://doi.org/10.1016/j.polymer.2012.06.039
[30] Usuki A, Kojima Y, Kawasumi M, Okada A, Fukushima Y, Kurauchi T, Kamigaito O. Synthesis of nylon 6-clay hybrid. Journal of Materials Research. 1993;8(5):1179-84.. https://doi.org/10.1557/JMR.1993.1179
[31] Cricrì G, Garofalo E, Naddeo F, Incarnato L. Stiffness constants prediction of nanocomposites using a periodic 3D-FEM model. Journal of Polymer Science Part B: Polymer Physics. 2012;50(3):207-20. https://doi.org/10.1002/polb.23001
[32] Gupta P, Chawla V, Jain V, Angra S. Green operations management for sustainable development: An explicit analysis by using fuzzy best-worst method. Decision Science Letters. 2022;11(3):357-66. https://doi.org/10.5267/j.dsl.2022.1.003
[33] Yung KC, Wang J, Yue TM. Modeling Young's modulus of polymer-layered silicate nanocomposites using a modified Halpin-Tsai micromechanical model. Journal of reinforced plastics and composites. 2006;25(8):847-61. https://doi.org/10.1177/0731684406065135
[34] Budiansky B. On the elastic moduli of some heterogeneous materials. Journal of the Mechanics and Physics of Solids. 1965;13(4):223-7. https://doi.org/10.1016/0022-5096(65)90011-6
[35] Mori T, Tanaka K. Average stress in matrix and average elastic energy of materials with misfitting inclusions. Actametallurgica. 1973;21(5):571-4. https://doi.org/10.1016/0001-6160(73)90064-3
[36] Benveniste Y. A new approach to the application of Mori-Tanaka's theory in composite materials. Mechanics of materials. 1987;6(2):147-57. https://doi.org/10.1016/0167-6636(87)90005-6
[37] Hill R. A self-consistent mechanics of composite materials. Journal of the Mechanics and Physics of Solids. 1965;13(4):213-22. https://doi.org/10.1016/0022-5096(65)90010-4
[38] Lielens G. (1999). Micro-macro modeling of structured materials, PhD thesis. UniversiteCatholique de Louvain, Louvain-la-Neuve, Belgium.
[39] Tucker III CL, Liang E. Stiffness predictions for unidirectional short-fiber composites: review and evaluation. Composites science and technology. 1999;59(5):655-71. https://doi.org/10.1016/S0266-3538(98)00120-1
[40] Huang ZM. Simulation of the mechanical properties of fibrous composites by the bridging micromechanics model. Composites Part A: applied science and manufacturing. 2001;32(2):143-72. https://doi.org/10.1016/S1359-835X(00)00142-1

[41] Huang ZM. Micromechanical prediction of ultimate strength of transversely isotropic fibrous composites. International journal of solids and structures. 2001;38(22-23):4147-72. https://doi.org/10.1016/S0020-7683(00)00268-7
[42] Dixit S, Padhee SS. Finite element analysis of fiber reinforced hybrid composites. Materials Today: Proceedings. 2019;18:3340-7. https://doi.org/10.1016/j.matpr.2019.07.255
[43] Potluri R, Paul KJ, Prasanthi P. Mechanical properties characterization of okra fiber based green composites & hybrid laminates. Materials Today: Proceedings. 2017;4(2):2893-902. https://doi.org/10.1016/j.matpr.2017.02.170
[44] Heydari-Meybodi M, Saber-Samandari S, Sadighi M. A new approach for prediction of elastic modulus of polymer/nanoclay composites by considering interfacial debonding: experimental and numerical investigations. Composites science and technology. 2015;117:379-85. https://doi.org/10.1016/j.compscitech.2015.07.014
[45] Muc A, Jamróz M. Homogenization models for carbon nanotubes. Mechanics of Composite Materials. 2004;40(2):101-6. https://doi.org/10.1023/B:MOCM.0000025484.92674.89
[46] Wang Y, Huang Z. A review of analytical micromechanics models on composite elastoplasticbehaviour. Procedia engineering. 2017;173:1283-90.. https://doi.org/10.1016/j.proeng.2016.12.159
[47] Younes R, Hallal A, Fardoun F, Chehade FH. Comparative review study on elastic properties modeling for unidirectional composite materials. Composites and their properties. 2012;17:391-408.. https://doi.org/10.5772/50362
[48] Abaimov SG, Khudyakova AA, Lomov SV. On the closed form expression of the Mori-Tanaka theory prediction for the engineering constants of a unidirectional fiber-reinforced ply. Composite Structures. 2016;142:1-6.. https://doi.org/10.1016/j.compstruct.2016.02.001
[49] Hill R. Theory of mechanical properties of fibre-strengthened materials-III. Self-consistent model. Journal of the Mechanics and Physics of Solids. 1965;13(4):189-98.. https://doi.org/10.1016/0022-5096(65)90008-6
[50] Chou TW, Nomura S, Taya M. A self-consistent approach to the elastic stiffness of short-fiber composites. Journal of Composite Materials. 1980;14(3):178-88. https://doi.org/10.1177/002199838001400301
[51] Huang ZM, Zhang YZ, Kotaki M, Ramakrishna S. A review on polymer nanofibers by electrospinning and their applications in nanocomposites. Composites science and technology. 2003;63(15):2223-53. https://doi.org/10.1016/S0266-3538(03)00178-7
[52] Huang ZM, Ramakrishna S. Micromechanical modeling approaches for the stiffness and strength of knitted fabric composites: a review and comparative study. Composites Part A: applied science and manufacturing. 2000;31(5):479-501. https://doi.org/10.1016/S1359-835X(99)00083-4
[53] Huang ZM. On micromechanics approach to stiffness and strength of unidirectional composites. Journal of Reinforced Plastics and Composites. 2019;38(4):167-96. https://doi.org/10.1177/0731684418811938
[54] Huang ZM, Zhou YX. Bridging Micromechanics Model. InStrength of Fibrous Composites 2011 (pp. 53-98). Springer, Berlin, Heidelberg. https://doi.org/10.1007/978-3-642-22958-9_3
[55] Dahlen C, Springer GS. Delamination growth in composites under cyclic loads. Journal of composite Materials. 1994;28(8):732-81. https://doi.org/10.1177/002199839402800803
[56] Ramakrishna S, Lim TC, Inai R, Fujihara K. Modified Halpin-Tsai equation for clay-reinforced polymer nanofiber. Mechanics of Advanced Materials and Structures. 2006;13(1):77-81. https://doi.org/10.1080/15376490500343824

[57] Genin GM, Birman V. Micromechanics and structural response of functionally graded, particulate-matrix, fiber-reinforced composites. International journal of solids and structures. 2009;46(10):2136-50.. https://doi.org/10.1016/j.ijsolstr.2008.08.010
[58] Alvinasab A. (2009). Nonlocal theory and finite element modeling of nano-composites. Ph.D. Dissertation, Clarkson University, New York.
[59] Giner E, Vercher A, Marco M, Arango C. Estimation of the reinforcement factor ξ for calculating the transverse stiffness E2 with the Halpin-Tsai equations using the finite element method. Composite Structures. 2015;124:402-8. https://doi.org/10.1016/j.compstruct.2015.01.008
[60] Halpin JC. Effects of Environmental Factors on Composite Materials. Air Force Materials Lab Wright-Patterson AFB OH; 1969 Jun 1. https://doi.org/10.21236/AD0692481
[61] Yung KC, Wang J, Yue TM. Fabrication of epoxy-montmorillonite hybrid composites used for printed circuit boards via in-situ polymerization. Advanced Composite Materials. 2006;15(4):371-84. https://doi.org/10.1163/156855106778835203
[62] Tsai SW, Hahn HT. Introduction to composite materials, Technomic Publishing Co. Inc, Washington University, Routledge, USA, 2018.
[63] Essabir H, Bensalah MO, Rodrigue D, Bouhfid R, Qaiss A. Structural, mechanical and thermal properties of bio-based hybrid composites from waste coir residues: Fibers and shell particles. Mechanics of Materials. 2016;93:134-44. https://doi.org/10.1016/j.mechmat.2015.10.018
[64] Thwe MM, Liao K. Effects of environmental aging on the mechanical properties of bamboo-glass fiber reinforced polymer matrix hybrid composites. Composites Part A: Applied Science and Manufacturing. 2002;33(1):43-52. https://doi.org/10.1016/S1359-835X(01)00071-9
[65] Hayashi T. On the improvement of mechanical properties of composites by hybrid composition. Proceedings of 8th International Reinforced Plastics Conference. 1972 (pp. 149-152).
[66] Zweben C. Tensile strength of hybrid composites. Journal of materials science. 1977;12(7):1325-37. https://doi.org/10.1007/BF00540846
[67] Patiño I, Isaza C. Mori-Tanaka-based statistical methodology to compute the effective Young modulus of polymer matrix nano-composites considering the experimental quantification of nanotubes dispersion and alignment degree. Engineering Solid Mechanics. 2022;10(1):79-98. https://doi.org/10.5267/j.esm.2021.9.002
[68] Kumar U, Rathi R, Sharma S. Carbon nano-tube reinforced nylon 6, 6 composites: a molecular dynamics approach. Engineering Solid Mechanics. 2020;8(4):389-96. https://doi.org/10.5267/j.esm.2020.2.002
[69] Barbero EJ. Introduction to Composite Materials Design (3rd Edition), Boca Raton, Florida, USA, 2018.
[70] Gloub GH, Van Loan CF. Matrix computations. Johns Hopkins Universtiy Press, (3rd edtion), Baltimore, Maryland, 1996.
[71] Huang J, Zhou J, Liu M. Interphase in polymer nanocomposites. JACS Au. 2022 Jan 13;2(2):280-91. https://doi.org/10.1021/jacsau.1c00430
[72] DeArmitt C. Functional fillers for plastics. In Applied plastics engineering handbook, New York, 2011:455-468. https://doi.org/10.1016/B978-1-4377-3514-7.10026-1